Heliyon 10 (2024) e34535

Contents lists available at ScienceDirect

Heliyon

journal homepage: www.cell.com/heliyon

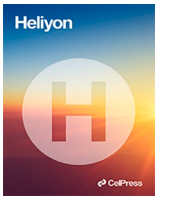

Research article

5-Fluorouracil resistance-based immune-related gene signature for COAD prognosis

Haixia Yan [a], Qinling Ou [a], Yonglong Chang [a], Jinhui Liu [b], Linzi Chen [a], Duanyang Guo [b], Sifang Zhang [a,*]

[a] *Department of Integrated Traditional Chinese & Western Medicine, The Second Xiangya Hospital, Central South University, Changsha, Hunan, 410011, China*

[b] *College of Integrated Traditional Chinese & Western Medicine, Hunan University of Traditional Chinese Medicine, Changsha, Hunan, 410208, China*

ARTICLE INFO

Keywords:
Colon adenocarcinoma
5-FU-Related genes
Gene signature
Prognostic model
Immune infiltration
5FRRDEGs

ABSTRACT

Background: Drug resistance is the primary obstacle to advanced tumor therapy and the key risk factor for tumor recurrence and death. 5-Fluorouracil (5-FU) chemotherapy is the most common chemotherapy for individuals with colorectal cancer, despite numerous options.

Methods: The Gene Expression Omnibus database was utilized to extract expression profile data of HCT-8 human colorectal cancer wild-type cells and their 5-FU-induced drug resistance cell line. These data were used to identify 5-FU resistance-related differentially expressed genes (5FRRDEGs), which intersected with the colorectal adenocarcinoma (COAD) transcriptome data provided by the Cancer Genome Atlas Program database. A prognostic signature containing five 5FRRDEGs (*GOLGA8A*, *KLC3*, *TIGD1*, *NBPF1*, and *SERPINE1*) was established after conducting a Cox regression analysis. We conducted nomogram development, drug sensitivity analysis, tumor immune microenvironment analysis, and mutation analysis to assess the therapeutic value of the prognostic qualities.

Results: We identified 166 5FRRDEGs in patients with COAD. Subsequently, we created a prognostic model consisting of five 5FRRDEGs using Cox regression analysis. The patients with COAD were divided into different risk groups by risk score; the high-risk group demonstrated a worse prognosis than the low-risk group.

Conclusion: In summary, the 5FRRDEG-based prognostic model is an effective tool for targeted therapy and chemotherapy in patients with COAD. It can accurately predict the survival prognosis of these patients as well as to provide the direction for exploring the resistance mechanism underlying COAD.

1. Introduction

Colorectal cancer (CRC) is one of the most common human malignancies; it is associated with high morbidity and mortality [1]. Its early symptoms are only noticeable in its late stages; thus, CRC incidence previously increased with age. However, the incidence in young adults has increased rapidly. Its primary treatment options—surgery, radiotherapy, and chemotherapy—can improve life

* Corresponding author.
E-mail address: sifangzhang2005@csu.edu.cn (S. Zhang).

https://doi.org/10.1016/j.heliyon.2024.e34535
Received 21 February 2024; Received in revised form 29 June 2024; Accepted 11 July 2024
Available online 14 July 2024

expectancy [2,3]. Approximately 80 % of patients with CRC are suitable for surgery; nonetheless, the prognosis is not excellent and only 40 % of the patients can be cured [4]. Colorectal adenocarcinoma (COAD) is the most prevalent histological subtype of CRC; it is highly aggressive and primarily affects the intestinal mucosa [5]. Researchers have achieved substantial progress in its diagnosis and treatment; however, the majority of cases are identified in the late stages. Moreover, patients with COAD demonstrate a dismal survival rate (only 14 %) [6,7]. The majority of terminal patients receive treatment primarily through chemotherapy and targeted therapy, which can only marginally prolong their overall survival because of drug resistance during the therapies [8]. Drug resistance develops over a complicated process that is primarily mediated by genetic abnormalities. Therefore, to explore novel treatment hypotheses and techniques to overcome drug resistance, researchers should identify the differentially expressed genes (DEGs) associated with drug resistance and investigate their association with drug sensitivity.

In patients with CRC, 5-FU is a crucial part of systemic chemotherapy. Despite encouraging developments in CRC treatment, the patients demonstrate low response rates. Additionally, the emergence of chemical resistance frequently undermines the advantages of 5-FU-based therapy [9]. Cancer cells exhibit two types of resistance to 5-FU-based therapies as follows: (i) primary resistance (innate) and (ii) secondary resistance (acquired). Both primary and secondary drug resistances include numerous molecular pathways [10]. Thymidylate synthases (TS) are the fundamental enzymes in 5-FU metabolism. Similar to other enzymes involved in 5-FU metabolism,

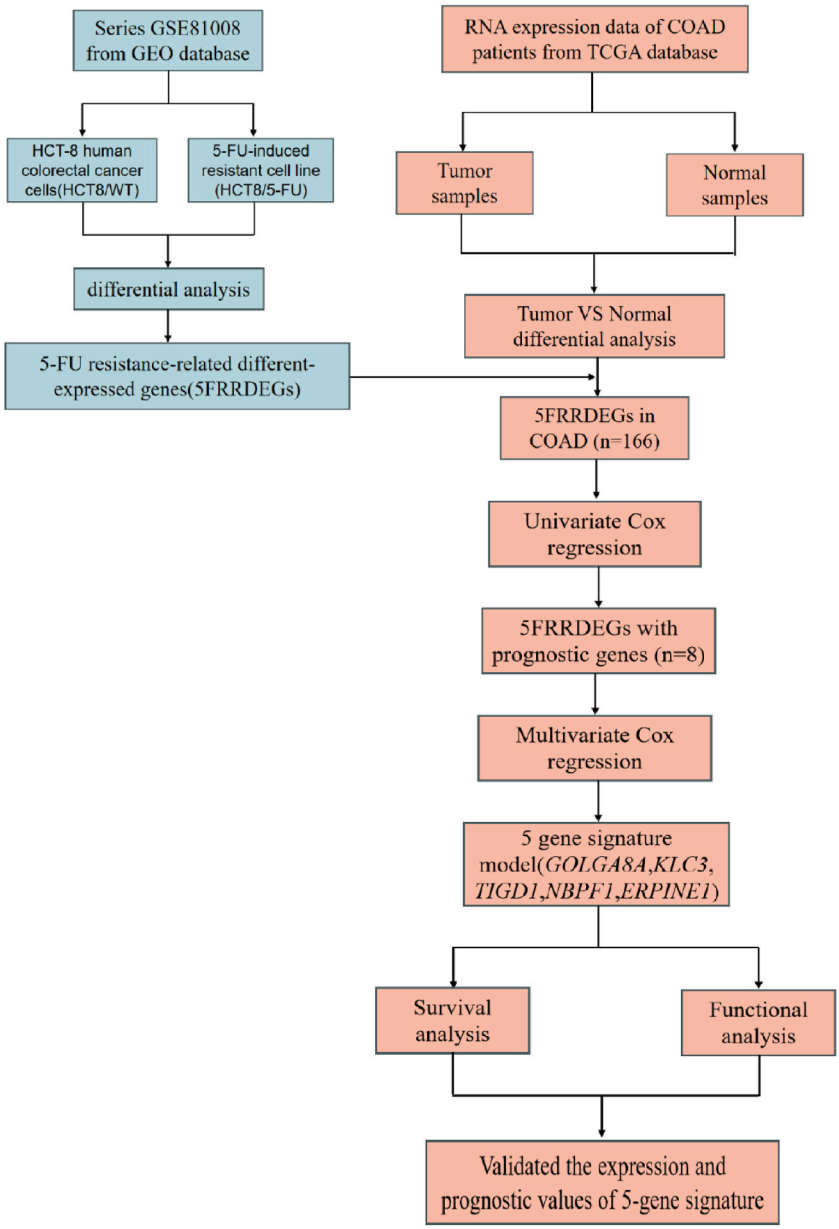

Fig. 1. The flow chart of this article.

TS is frequently modified to enhance 5-FU resistance [11]. Additionally, the expression of long non-coding RNAs affects 5-FU drug resistance [11]. High programmed cell death 4 (*PDCD4*) can prevent the CRC cells from proliferating and increase their susceptibility to 5-FU, whereas low *PDCD4* can promote their apoptosis [12,13]. Few researchers have examined the function of 5FRRDEGs in predicting prognosis and clinicopathology in patients with COAD, despite numerous studies on the mechanism underlying 5-FU resistance.

Tumor immunotherapy is being increasingly considered as a viable treatment strategy; nevertheless, the tumor immune milieu is central to the antitumor effects of immunotherapy. Therefore, the anatomical immune microenvironment is relevant for tumor therapy. Through the secretion of several cytokines, chemokines, and other substances, cancer cells can functionally modify their microenvironment [14]. Thoroughly examining the complexity of the tumor immune microenvironment (TIME) may facilitate determining sophisticated biomarkers useful in identifying novel targets for therapeutic modulation [14,15]. Targeting TIME has advantages over cancer cells because of the instability of the cancer cell genome, which can lower immunological surveillance and reduce drug resistance recurrence [16–18]. To discover more effective treatment options, researchers should establish the association between TIME and 5-FU resistance in patients with COAD.

Progress in genomics has facilitated assessing numerous samples at a lower cost, in less time, and with fewer efforts [19–21]. Thus, we identified the DEGs between human colorectal cancer wild-type cells (HCT8/WT cells) and their 5-FU-induced drug resistance cell line (HCT8/5-FU cells) using bioinformatics, i.e., 5FRRDEGs.The HCT8/5-FU cells are 5-FU resistant cells induced by 5-FU to HCT/WT cells. Moreover, we examined their association with the prognosis and TIME and investigated novel therapeutic strategies.

In this study, 5FRRDEGs were identified, and their functional enrichment analysis was conducted using the Genomic Spatial Event (GSE) gene chip (GSE81008) expression data of both HCT8/WT cells and HCT8/5-FU cells from the Gene Expression Omnibus (GEO) database. Regression analysis was conducted to develop a predictive gene model after intersecting with DEGs of the patients with COAD from The Cancer Genome Atlas Program (TCGA). We confirmed the association of the 5FRRDEGs with immune infiltration and immunological checkpoints. Fig. 1 illustrates the study process. Our findings will offer diagnostic and treatment options for individuals resistant to 5-FU therapy.

2. Materials and methods

2.1. 5FRRDEG screening

The GEO database (https://www.ncbi.nlm.nih.gov/geo/) was accessed to collect the expression profile data of GSE81008 for both HCT8/WT cells and HCT8/5-FU cells. The DEGs were identified using "limma" (version 3.54.2), with a threshold of log2-fold change (FC) $\geq$1 and an adjusted *P*-value $<$0.05. We aimed to discover 5FRRDEGs that exhibit significantly different expressions across these two types of cells.

2.2. Functional enrichment analysis

To determine the potential function of 5FRRDEGs, Gene Set Enrichment Analysis (GSEA) was conducted using the "clusterProfiler" package. The first 12 substantial signaling pathways were selected for display, and the threshold of the pathway was set to a *P*-value $<$0.05.

2.3. Identifying DEGs in patients with COAD

After downloading the gene expression profile data and associated clinical information from TCGA (https://portal.gdc.cancer.gov/), 474 COAD samples and 41 healthy tissue samples were utilized for a differential analysis using the "DEseq2" software. An absolute FC $\geq$ 1 and an adjusted *P*-value $<$0.05 were used to define the DEG threshold. TCGA data are publicly accessible, and the study adhered closely to its access policies and publication standards. Therefore, no ethical review or committee permission was required for this research.

2.4. Establishing and validating a prognostic predictive signature

First, to identify the DEGs related to drug resistance in COAD, the "ggvenDiagram" used the intersection of DEGs in COAD and 5FRRDEGs. Genes with a *P*-value $<$0.05 were considered statistically significant. Second, a univariate Cox regression analysis was conducted using the "survival" package to determine the overall survival (OS)-related genes in patients with COAD. Establishing a prognostic model involved a multivariate Cox regression analysis of the selected genes. To calculate the risk score, the gene expression level (Expi) and regression coefficient (coei) of the model were combined linearly based on the genes screened by cox regression analysis. The risk score of each patient was calculated as follows [22,23]:

$$Risk\ score = \sum_{I=1}^{N} (Expi * coei)$$

Based on a median risk score, the patients were split into two groups as follows: high- and low-risk groups [24]. The prediction power of the prognostic characteristics for OS was assessed using the Kaplan–Meier survival curve [25] and time-dependent receptor

operating characteristic (ROC) curve [26].

2.5. Constructing and evaluating a predictive nomogram

Univariate and multivariate Cox analyses were conducted to compare the five genetic features with other clinical traits, such as the Tumor, Node, Metastasis stage, age, and sex, to confirm their independence in predicting the OS in patients with COAD [27]. A *P*-value <0.05 indicated statistical significance [28]. We obtained the 95 % confidence interval and hazard ratio for each factor. Utilizing the risk score and clinical data, we created a predictive nomogram as a quantitative analysis tool to estimate the survival risk of patients with COAD [29].

2.6. Mutation data processing

The "TCGAmutations" R package was used to obtain the mutation data from TCGA. The "maftools" R package was used to analyze the data and create a waterfall map. Tumor mutational burden (TMB) difference and survival analyses were conducted to examine the accuracy of the prognostic model and determine the impact of TMB.

2.7. Predicting chemotherapeutic response

Chemotherapy response was evaluated in high- and low-risk patients with COAD using the R package "oncoPredict". Based on a 50 % inhibiting concentration (IC50) for each patient, the results were determined using the Genomics of Drug Sensitivity in Cancer (GDSC) website (https://www.cancerrxgene.org/).

2.8. Assessing immune cell infiltration

"ssGSEA" was used to measure the immune cells in the two risk groups and observe the distinct immune-related function between the high and low-risk groups. We estimated immune cell infiltration in the patients with COAD based on the risk ratings using different R packages to investigate its association with the five gene characteristics. Additionally, we computed the correlation between the immune cell subtype infiltration levels and 5FRRDEGs using the Data mining of the Tumor Immune Estimation Resource (TIMER) database (http://cistrome.org/TIMER/).

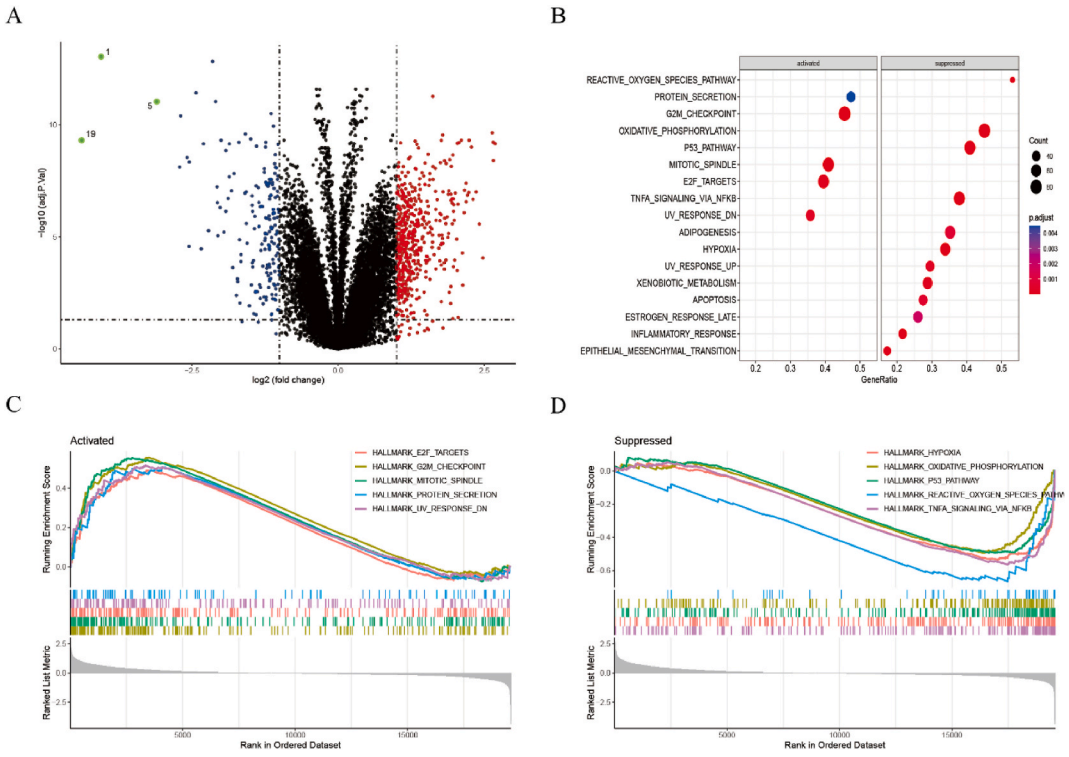

Fig. 2. (A) Volcano figure of difference analysis of 5-FU resistant and non-resistant cells. (B) Bubble diagram of the GSEA of 5FRRDEGs. (C) Gsearank plot of the activated pathway. (D) Gsearank plot of the suppressed pathway.

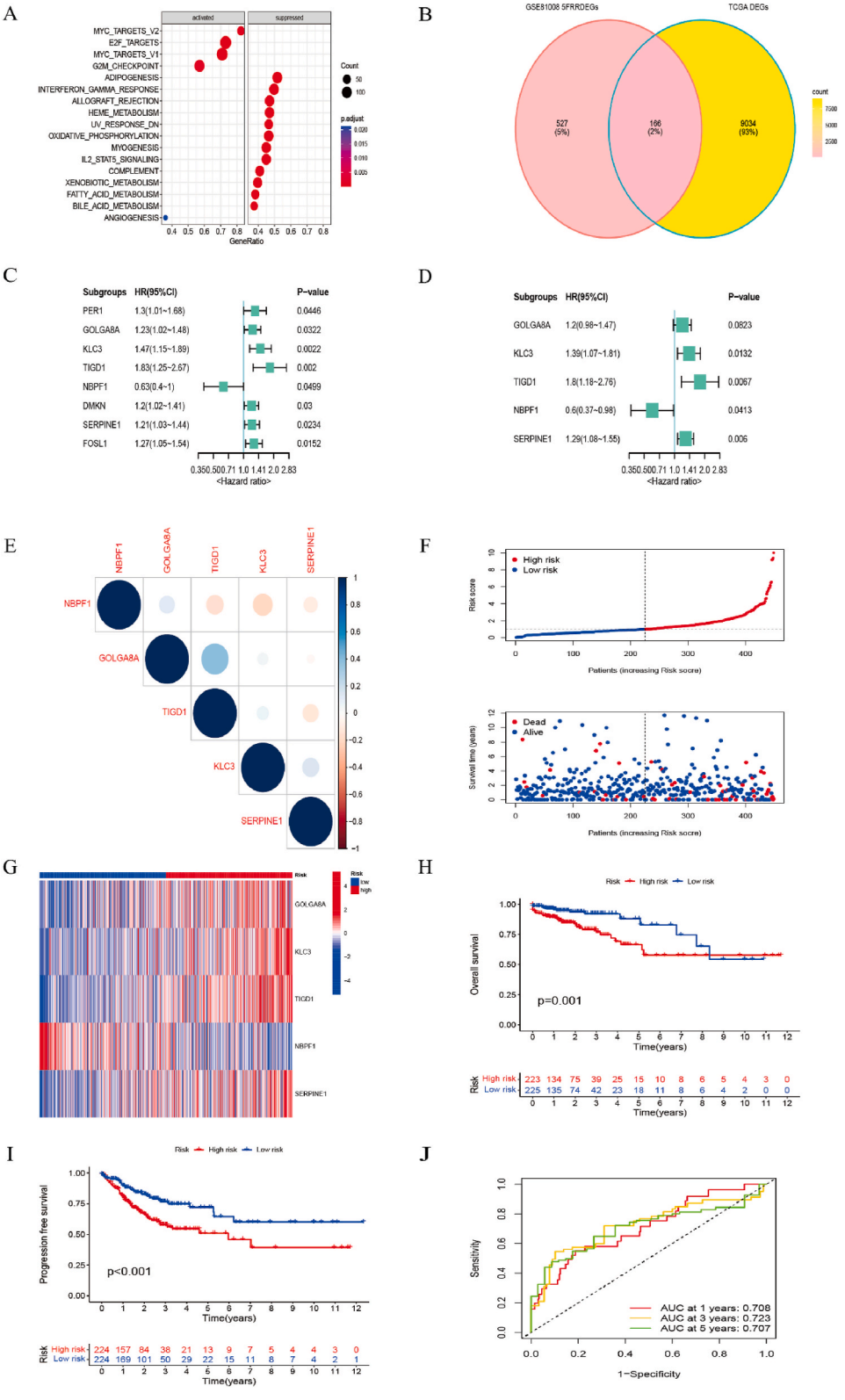

(caption on next page)

Fig. 3. (A) Bubble diagram of the GSEA of DEGs in COAD. (B)Venn diagram of the 5FRRDEGs and DEGs of COAD. (C) 5FRRDEGs in COAD associated with prognosis are predicted using the univariate Cox regression analysis. (D) Prediction models are constructed using the multivariate Cox regression analysis. Forest plot of the 5FRRDEGs with prognostic effect. (E) Corrplot of the 5FRRDEGs with prognostic effect. (F) Prognosis of the risk signature for patients with COAD. Distribution of the survival risk scores, survival condition, and survival time in the high-low risk groups. (G) Heatmaps of the expression of five 5FRRDEGs. (H) Overall survival curve; the OS of the high-risk group is low. *P*-value <0.05 indicates statistical significance. (I) KM curve of PFS in the high- and low-risk groups. (J) The ROC curve confirms the ability of the model to predict the 1- to 3-year survival rate. AUC values are >0.05, indicating a highly accurate signature.

2.9. Single cell data analysis

To identify the expression of 5FRRDEGs in single-cell data, we acquired the CRC single-cell data GSE161277 from the GEO database.

3. Results

3.1. Identification and functional enrichment analysis of 5FRRDEGs

Using the GSE81008 dataset from the GEO database, DEGs in gene expression profiles between the HCT8/WT cells and HCT8/5-FU cells were examined. Using $P < 0.05$ and $|\log2\ FC| \geq 1$ as the threshold, 693 5FRRDEGs were examined. Of them, 508 were upregulated, whereas 185 were downregulated. The colors black, red, blue, and green denote undifferentiated, upregulated genes, downregulated, and downregulated genes with high difference multiples. The dashed line denotes the boundary between DEGs and undifferentiated genes (Fig. 2A, Supplemental Table 1). Utilizing the GSEA enrichment pathway analysis, we investigated the application of 5FRRDEGs. 5FRRDEGs are active in tumor-related protein secretion, G2M checkpoint, mitotic spindle, E2F targets, and ultraviolet response in DNA pathways. The larger the circle, the more genes are enriched in this pathway; the redder the color, the greater the enrichment. The percentage of DEGs in the reference genes is indicated by GeneRatio (Fig. 2B, C, and D). The G2/M checkpoint is used by cancer cells to evade genotoxic anti-cancer therapy by repairing DNA before cell division [30]. Tumor therapy-induced medication resistance can be

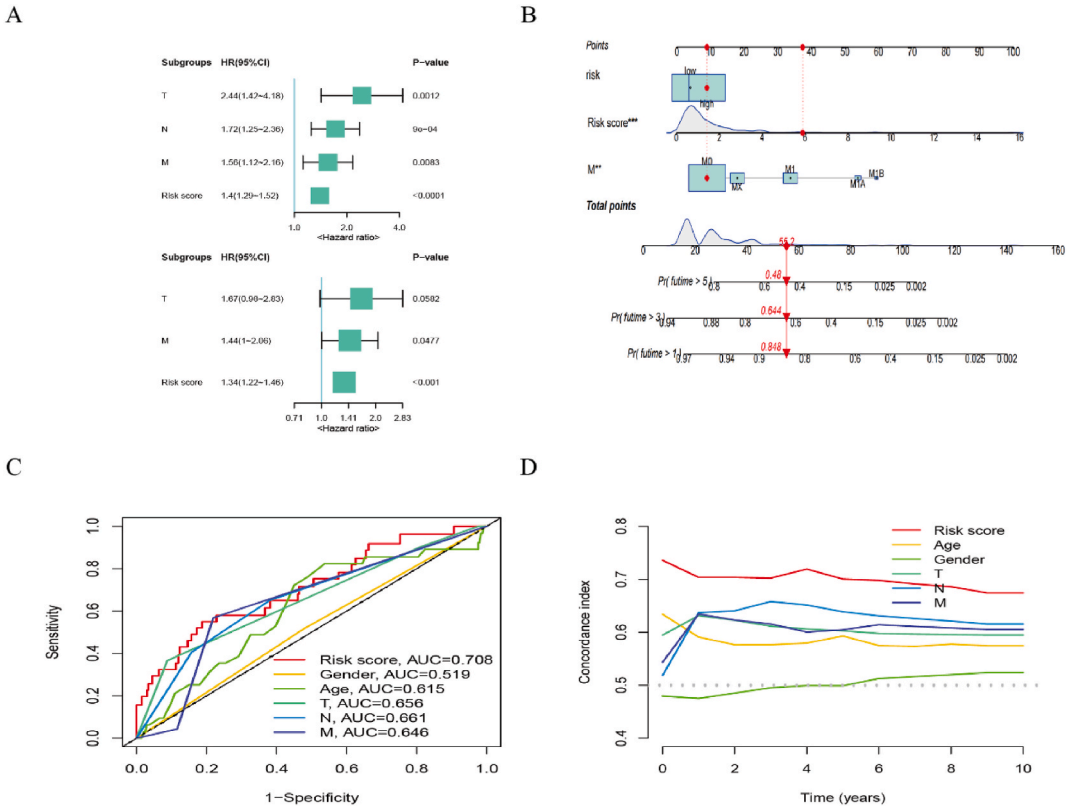

Fig. 4. Verifying the feasibility of predicting the OS and independent prognosis using the risk model related to 5FRRDEGs. (A) Univariate and multivariate Cox regression analyses. The risk score and stage can estimate the OS. The risk score can independently predict the OS of patients with statistical significance. (B) Nomogram model to forecast the survival probability of a patient based on clinical factors. (C) Comparison of time-dependent ROC curves of the nomograms for the 1-year OS in patients with COAD. (D) Time-dependent C-index of the prognostic model.

overcome by focusing on the mitotic regulators [31]. Targeting the genes associated with the E2F pathway can help overcome drug resistance to radiation and chemotherapy. This is because pathway activation causes drug resistance [32,33]. Some of the genes in 5FRRDEGs have been studied in relation to drug resistance in tumors, such as metastasis associated with colon cancer 1(MACC1), AXL and so on. The increased expression of MACC1 facilitated the growth and strengthened the resistance of CRC cells to irinotecan [34]. According to recent research, AXL may be a viable target for anti-cancer medication therapy since it can reduce drug resistance in cancer cells [35]. Thus, 5FRRDEGs are crucial to the development of malignant transformation in COAD.

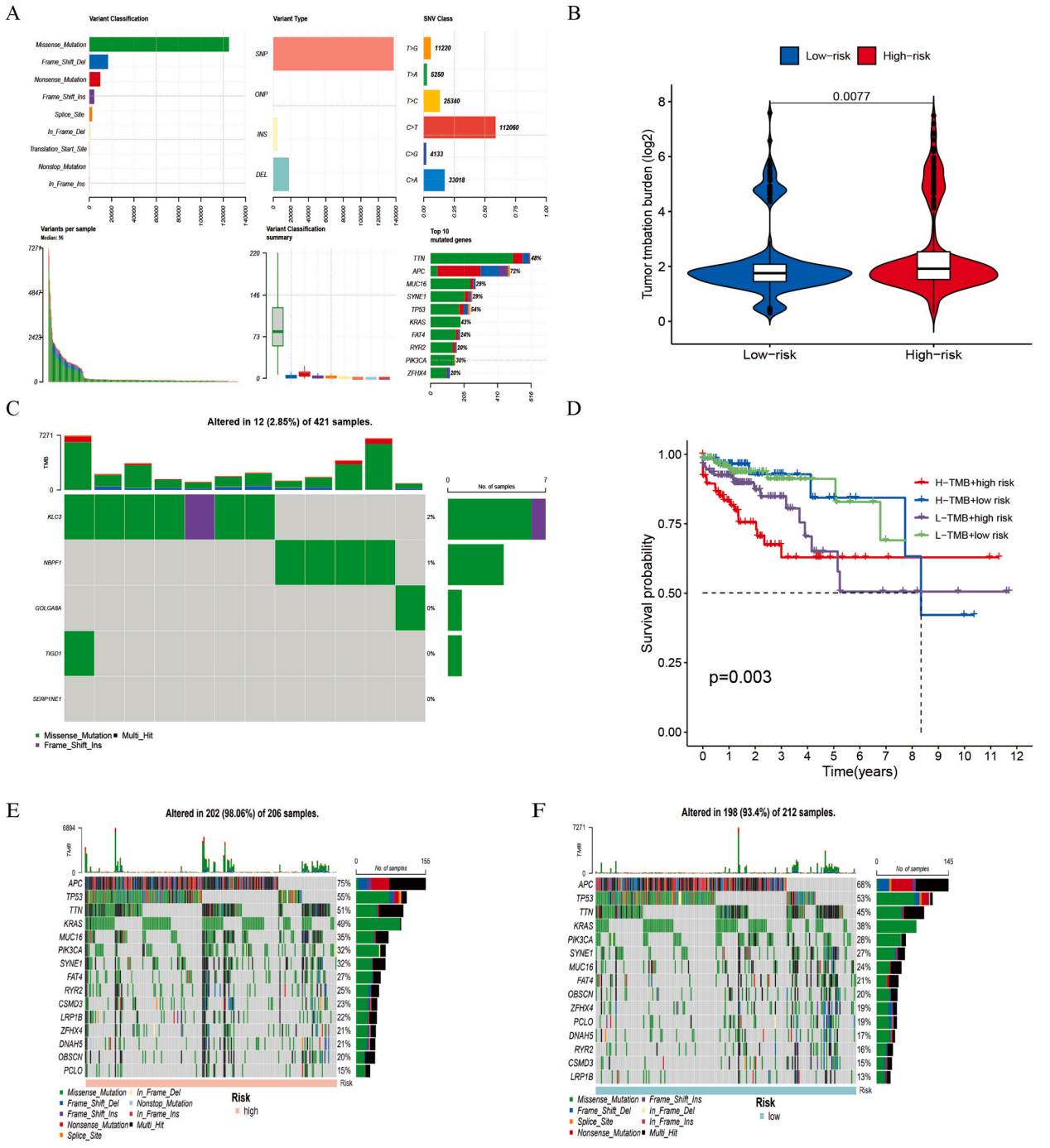

Fig. 5. (A) Mutations in the patients with COAD from the TCGA cohort and a mutation landscape map of the patients. (B) TMB in the high- and low-risk groups. (C) Somatic mutation characteristics of the five genes in patients with COAD. (D) KM curves of the four groups divided by the TMB combined risk ($P < 0.05$). (E, F) Somatic mutation characteristics in the high- and low-risk categories are depicted in a waterfall diagram.

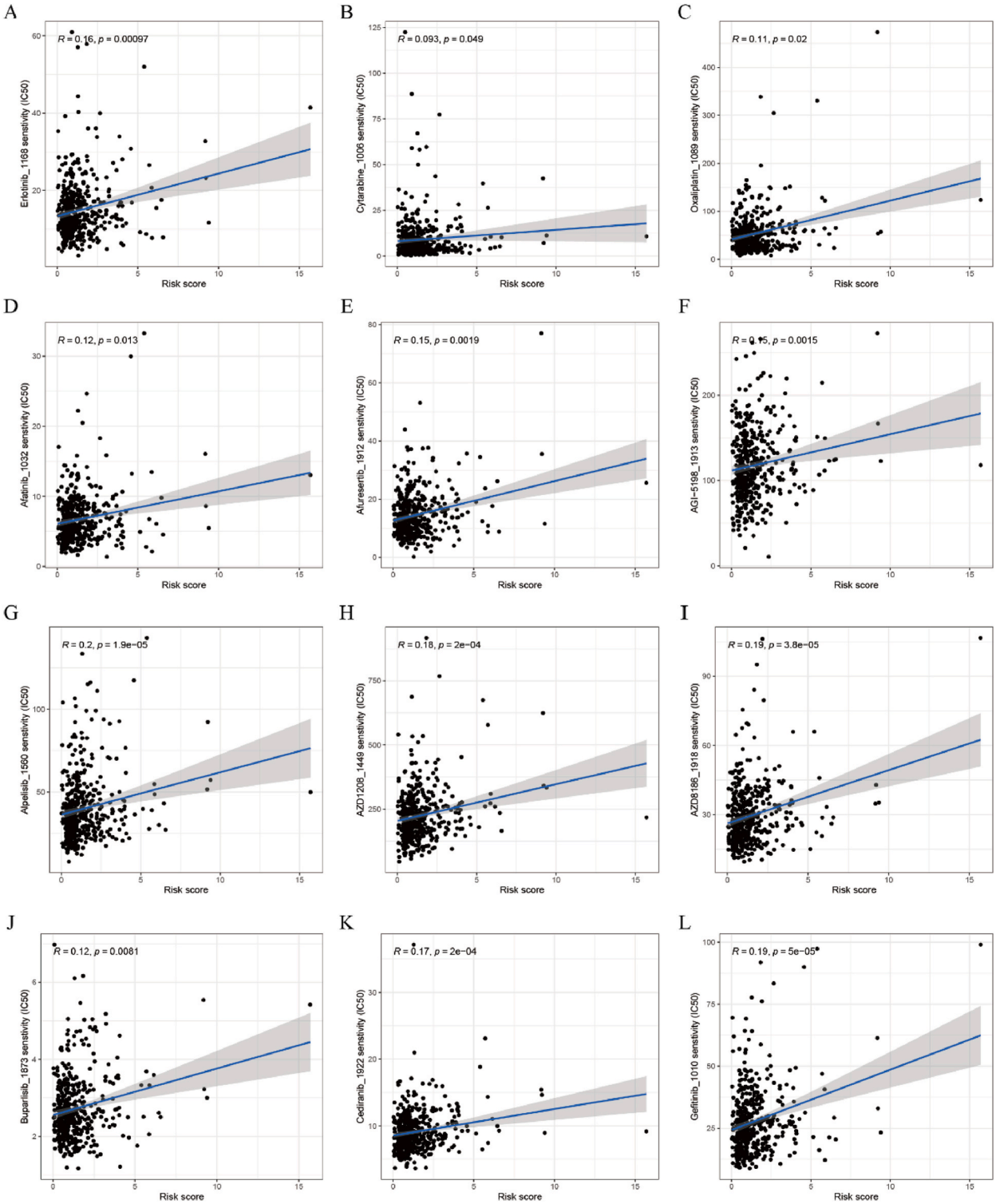

Fig. 6. Drug sensitivity concerning the risk group for (A) erlotinib, (B) cytarabine, (C) olaparib, (D) afatinib, (E) afuresertib, (F) AGI-5198, (G) alpelisib, (H) AZD1208, (I) AZD8186, (J) buparlisib, (K) cediranib, and (L) gefitib.

3.2. Constructing and validating prognostic features using 5FRRDEGs

TCGA was used to identify DEGs between COAD and healthy tissue samples; subsequently, GSEA enrichment analysis was conducted. The MYC targets, E2F targets, and G2M checkpoint pathways were activated, whereas some metabolism-related pathways were inhibited (Fig. 3A). A total of 166 genes intersected with the DEGs in COAD (Fig. 3B). We conducted a univariate Cox regression analysis, selected genes with *P*-values <0.05, and identified eight 5FRRDEGs with prognostic values (Fig. 3C–Supplementary Table 2). Additionally, we identified the 5FRRDEGs with the highest prognostic value using a progressive multivariate Cox regression analysis for these eight genes and their association with OS in patients with COAD. Of the 166 intersecting genes, *GOLGA8A*, *KLC3*, *TIGD1*, *NBPF1*, and *SERPINE1* were finally selected (Fig. 3D). Subsequently, we assessed the association between each gene in the model. *NBPF1* was negatively correlated with both *TIGD1* and *KLC3*, whereas *GOLGA8A* was positively correlated with *TIGD1* (Fig. 3E). We developed a risk score model using the expression of these five genes as follows: Risk score = (0.1814***GOLGA8A* expression) + (0.3320***KLC3* expression) + (0.5887***TIGD1* expression) + (−0.5092***NBPF1* expression) + (0.2559***SERPINE1* expression) (Supplementary Table 3). The patients with COAD were split into two groups—high- and low-risk groups—using the median as the critical value. The risk score of the patients who died from COAD was higher than that of the patients who survived (Fig. 3F). A heatmap was used to display the expressions of the five 5FRRDEGs. The high-risk group demonstrated high *GOLGA8A*, *KLC3*, *TIGD1*, and *SERPINE1* expressions and low *NBPF1* expression (Fig. 3G). The Kaplan–Meier curves demonstrated a substantial association of the risk with the OS time and progression-free survival (PFS). The low-risk group demonstrated a longer OS time than the high-risk group (Fig. 3H and I). The area under the ROC (AUC) values for 1, 3, and 5 years were 0.708, 0.723, and 0.707, respectively, indicating good model performance in predicting the survival time (Fig. 3J).

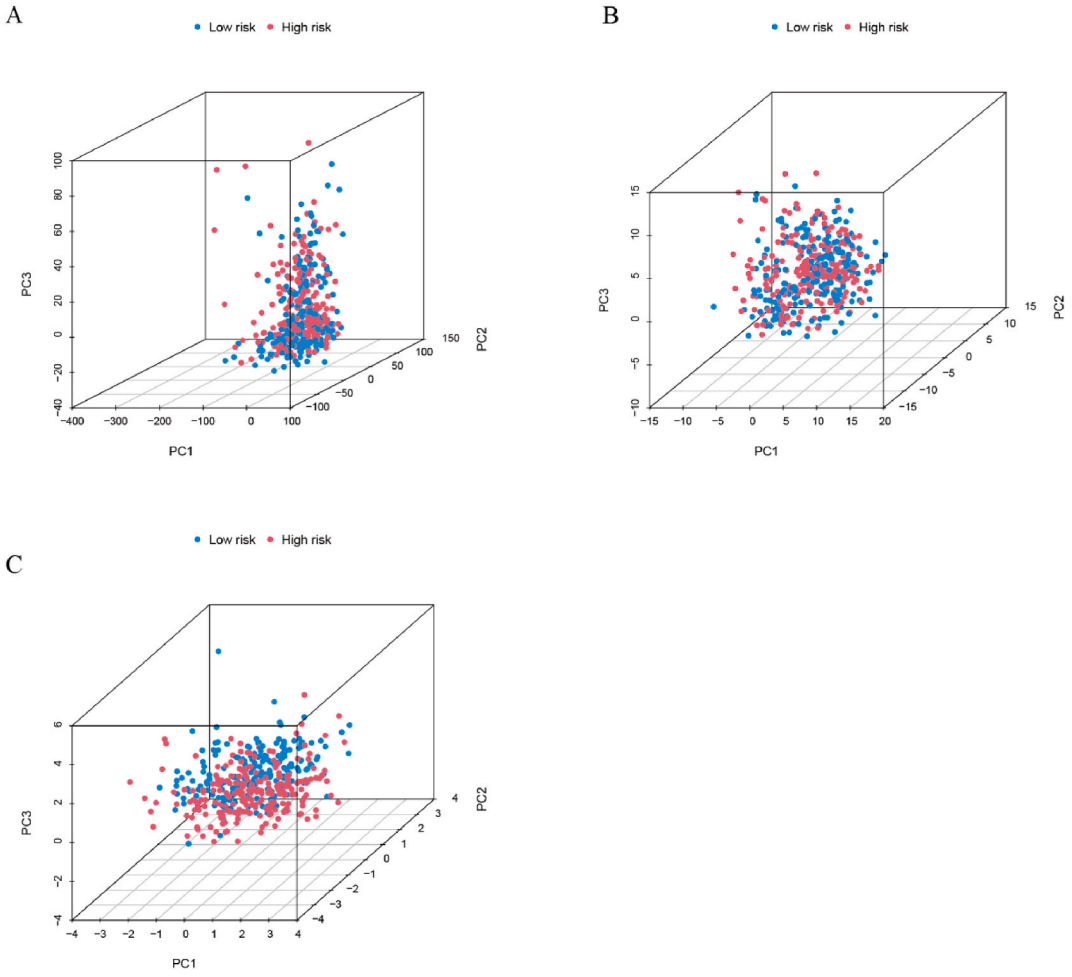

Fig. 7. (A–C) PCA in the high- and low-risk groups. (A) PCA of DEGs between COAD and healthy tissue samples. (B) PCA of 5FRRDEGs. (C) PCA of model genes.

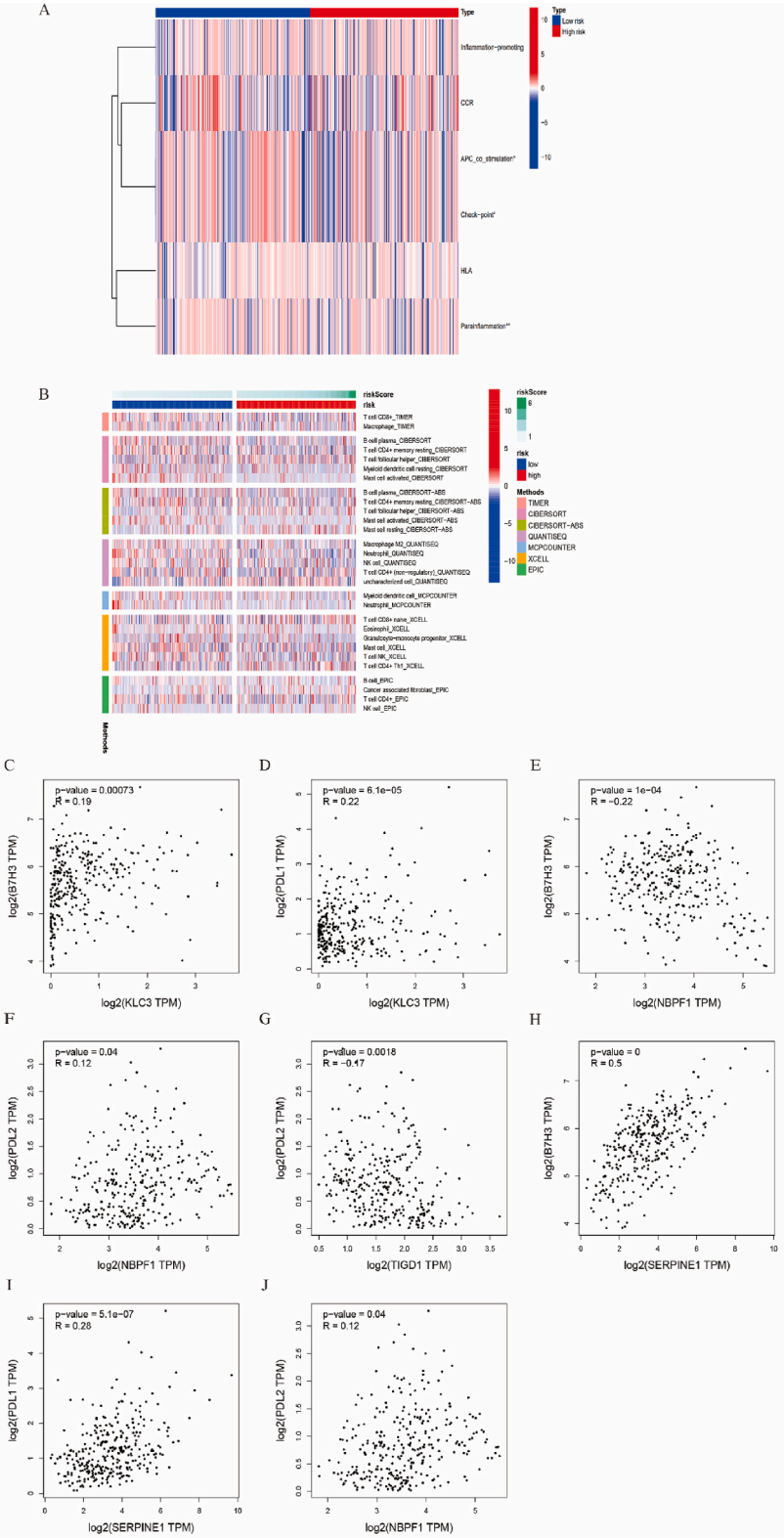

Fig. 8. (A) "ssGSEA" scores for the immunological cell and function in the high- and low-risk groups. (B) Heatmap of immune cell infiltration in the high- and low-risk groups. Correlation scatter plots of (C) *KLC3* and *B7H3*. (D) *KLC3* and *PDL1*. (E) *NBPF1* and *B7H3*. (F) *NBPF1* and *PDL2*. (G) *TIGD1* and *PDL2*. (H) *SERPINE1* and *B7H3*. (I) *SERPINE1* and *PDL1*. (J) *SERPINE1* and *PDL2*.

3.3. Constructing OS prediction nomogram in the TCGA cohort

The age, sex, risk score, and T (the condition of the primary tumor), N (the condition of regional lymph node), and M (the condition of metastasis) stages for Cox proportional risk regression were used to demonstrate that the risk model is an independent marker. The M stage ($P = 0.0477$, hazard ratio (HR) = 1.44, 95%CI = 1–2.06) and risk score ($P < 0.001$, HR = 1.34, 95%CI = 1.22–1.46) were associated with the OS in patients with COAD. Thus, the risk score is a prognostic factor for patients with COAD (Fig. 4A). We used the significant variables identified in the multivariate analysis to construct a prognosis nomogram that predicted patient survival reliably. The total scores of the M stage and risk score can be used to determine the survival rate for each patient at 1, 3, and 5 years (Fig. 4B). The model accuracy was assessed using the time-independent ROC curve. The prognostic model demonstrated a higher AUC value (0.708) than other clinical parameters (Typically, AUC values are between 0.5 and 1.0, with a larger AUC representing better performance.), demonstrating its strong predictive ability and its predictive power is superior to other clinical features (Fig. 4C). Furthermore, we assessed its accuracy using the C-index. The dotted line denoted 0.5, which was inconsistent and suggested no predictive power. These results indicated the superiority of our model over other medical variables (Fig. 4D).

3.4. Mutation in patients with COAD

We assessed the overall state of mutations by analyzing the COAD mutation data. The key types of COAD mutations identified were missense mutation and single nucleotide polymorphisms (SNP). C for T mutation demonstrated the highest frequency of base substitution than other base substitution types. Moreover, *TTN* and *APC* demonstrated the highest mutation frequency (Fig. 5A). We estimated the TMB of the patients to understand the included genetic mutations. The TMB of the high-risk group was greater than that of the low-risk group (Fig. 5B). The mutation frequency of these five genes was examined to comprehend their stability. These genes were largely stable (Fig. 5C). To explore the combined effects of the risk score and TMB, the median segmentation method was used. The patients were divided into high-TMB (H-TMB) and low-TMB (L-TMB) groups, patients as follows: H-TMB + high risk, H-TMB + low risk, L-TMB + high risk, and L-TMB + low risk. The H-TMB + high risk group demonstrated the lowest OS (Fig. 5D). We compared the leading 10 genes for the mutation frequency; the high-risk demonstrated had a greater mutation frequency than the low-risk group (Fig. 5E and F).

3.5. Predicting chemotherapeutic response

The "oncopredict" R package was used to investigate the effects of targeted treatment and chemotherapy on the high- and low-risk groups. Regardless of targeted medications or chemotherapy, the higher the risk score, the higher the IC50. Therefore, patients with low-risk scores benefited more than those with high-risk scores ($P < 0.05$). Analysis of the correlation between the risk score and the drug's IC50 was done. The correlation curve is shown by the blue line, and its confidence interval is indicated by the gray area (Fig. 6A–L).

3.6. Immunophenotypic traits of patients with COAD in the high- and low-risk groups

Principal component analysis (PCA) was conducted to examine the distributions of immunophenotypic differences in the high- and low-risk groups. Our prognostic model accurately identified the patients. We observed no discernible difference between the distribution of 5FRRDEGs and DEGs between COAD and healthy tissue samples (Fig. 7A and B). However, the 5FRRDEG risk model effectively differentiated between the high- and low-risk groups based on the phenotypic differences (Fig. 7C).

3.7. Immune landscapes of the low- and high-risk groups

"ssGSEA" was utilized to depict the distributions of immune-related functions and risk ratings. The immune-related functions, such as inflammation−promotion, CC chemokine receptor (CCR), antigen-presenting cells (APC)_co_stimulation, check−point, human leukocyte antigen (HLA), and parainflammation, were significantly different between the high- and low-risk groups (Fig. 8A). Parainflammation is central to disease progression [36,37]. CRC is substantially influenced by the gut microbiota. Moreover, endogenous mutations, epigenetic modifications, and increased pluripotency in the intestinal epithelial cells are supposedly caused by microbial parainflammation [38]. We examined the fraction of tumor immune cell types using multiple algorithms to examine the variations in immune cell infiltration between the high- and low-risk groups. The high-risk group demonstrated high T follicular helper cell and native $CD8^+$ cell infiltration levels. The low-risk group demonstrated a higher percentage of $CD8^+$ cells, macrophages, and natural killer (NK) cell infiltration (Fig. 8B). The checkpoints differ between the high- and low-risk groups. Thus, the common immunological checkpoints, namely programmed cell death ligand 1 (PDL1), programmed cell death ligand 2 (PDL2), and B7 homolog 3 protein (B7H3), were examined using the Gene Expression Profiling Interactive Analysis database (http://gepia2.cancer-pku.cn). *SERPINE1* was positively correlated with *B7H3*, *PDL1*, and *PDL2*. *KLC3* was positively correlated with *B7H3* and *PDL1*. *NBPF1* and *TIGD1* were positively correlated with *PDL2*. Additionally, *NBPF1* was negatively correlated with *B7H3* ($P < 0.05$) (Fig. 8C–J). Thus, the genetic signature may affect COAD prognosis through immune system interference.

3.8. Single-cell RNA-seq analysis

The uniform manifold approximation and projection approach, a method for reducing nonlinear dimensionality, was used to categorize various tumor-infiltrating cells (Fig. 9A). Moreover, the image displayed expressions of 5FRRDEGs in seven types of cells was displayed. *NBPF1* expressions were lower in the T cells and B cells (Fig. 9B), whereas *GOLGA8A* and *TIGD1* expressions were higher in the tumor-infiltrating cells (Fig. 9C and D). *SERPINE1* and *KLC3* expressions remained unchanged (Fig. 9E and F). Thus, 5FRRDEGs can affect the tumor microenvironment, which could influence tumor progression. These findings provide direction for the treatment of COAD.

3.9. Validating the prognostic potential internally and externally

We assessed the expression of these five genes between the tumor and normal intestinal tissues in a publicly accessible database to confirm the validity of our gene model (https://ualcan.path.uab.edu). Tumor tissues demonstrated substantially high mRNA levels of

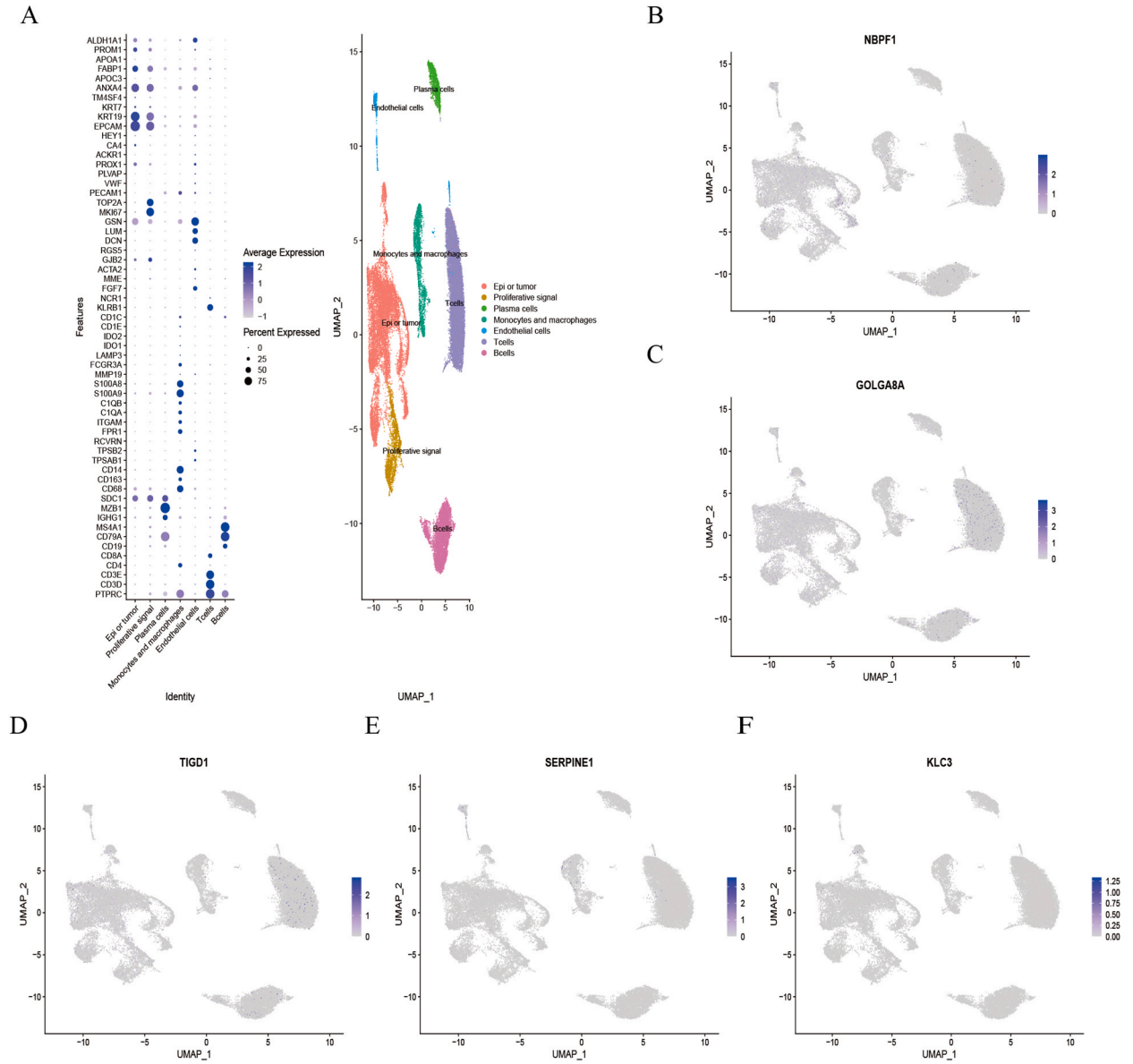

Fig. 9. Single-cell RNA-seq analysis displays numerous cell types in COAD and healthy tissue samples. (A) UMAP displays the key cell types (right). Representative markers across the major cell types are displayed in the bubble diagram (left). (B–F) Expressions of five genes (*NBPF1*, *GOLGA8A*, *TIGD1*, *SERPINE1*, and *KLC3*) in the model.

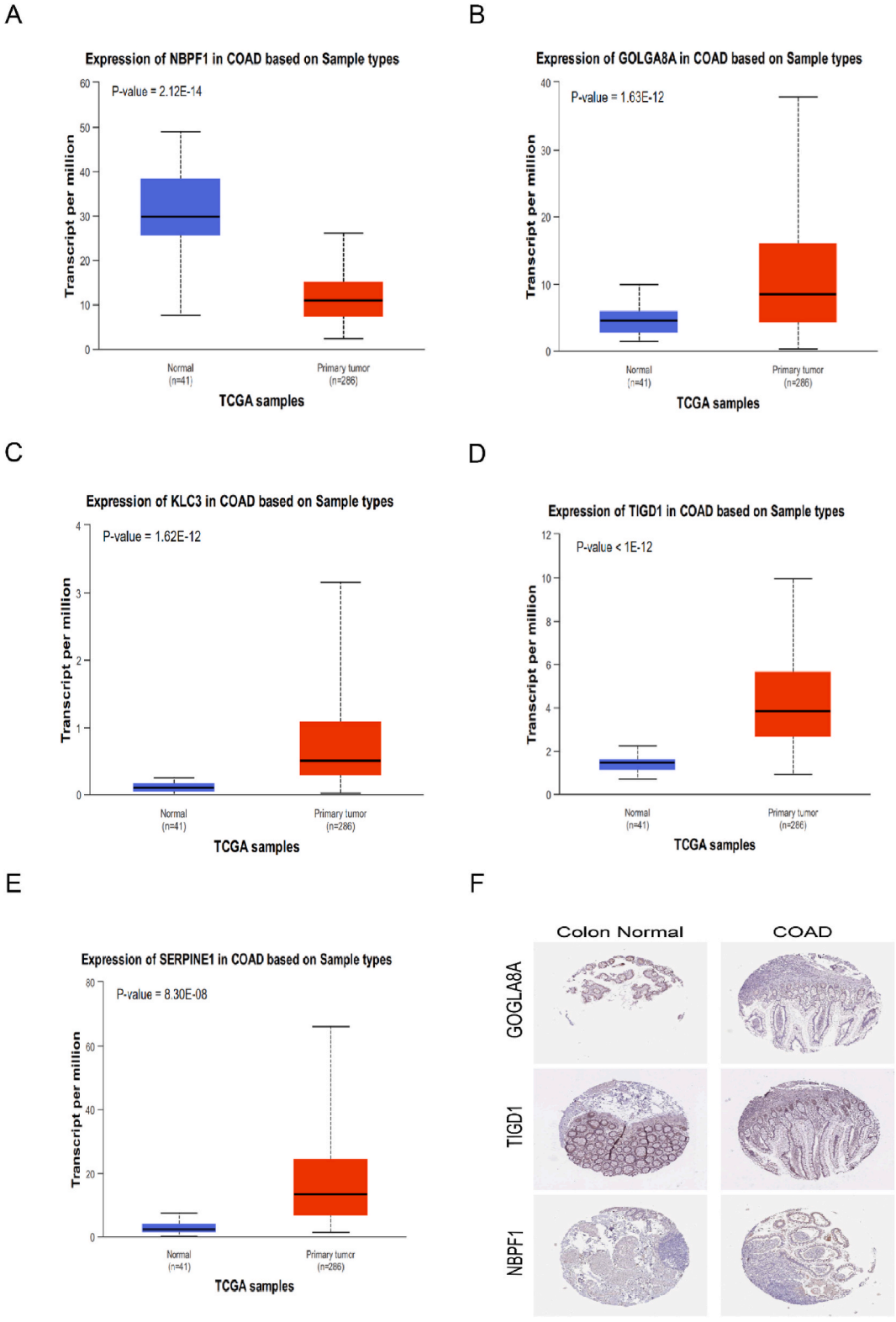

Fig. 10. Validating the expression of 5FRRDEGs in COAD. (A–E) Expressions of each gene in the TCGA cohort with 286 COAD and 41 healthy samples. (F) Expression of GOGLA8A, *TIGD1*, and *NBPF1* in COAD and healthy colon tissues.

GOLGA8A, *KLC3*, *TIGD1*, and *SERPINE1* and low levels of only *NBPF1*, compared with healthy intestinal tissues (Fig. 10A–E). Additionally, we examined the *GOLGA8A*, *TIGD1*, and *NBPF1* gene protein levels in clinical COAD and healthy specimens using the Human Protein Atlas (https://www.proteinatlas.org/). The results were in agreement with our findings of the mRNA study (Fig. 10F). Subsequently, we assessed the correlation between these gene expression and immune cell infiltration. NBPF was positively correlated with the B cells, CD8 T cells, CD4 T cells, macrophages, and neutrophils. By contrast, *SERPINE1* was positively correlated with B cells and negatively correlated with others (Figure S1A-E, http://cistrome.org/TIMER/).

4. Discussion

Antimetabolic medications halt the production of substances required for cell division. 5-FU is utilized in the initial stages of treatment as an antimetabolic drug for several tumors. It is a traditional chemotherapy medication used to treat CRC [39,40]. However, after 5-FU chemotherapy, the patients frequently present with signs of acquired or primary resistance [41]. 5-FU resistance is a complex phenomenon that includes mismatch repair problems, aberrant enzyme metabolism, transport issues, cell cycle disruptions, and apoptotic resistance. The molecular mechanisms underlying 5-FU resistance remain unclear, despite progress in biological research approaches [42]. Numerous gene models predict the prognosis of COAD after treatment. However, researchers have not explored the genes associated with 5-FU resistance and their implications for immunological prognosis. Thus, researchers should construct a gene model associated with 5-FU resistance that can accurately identify the patients at a high risk of developing 5-FU resistance [43]. This step will help patients with COAD gain benefits from effective therapies.

In this study, we conducted a gene chip analysis from the GEO database to identify 5FRRDEGs. After obtaining 693 5FRRDEGs, we conducted a GSEA enrichment analysis. They primarily activated the tumor cycle-related pathways, consistent with previous findings [44]. The DEGs of 5FRRDEGs and patients with COAD intersected. Subsequently, we conducted univariate and multivariate Cox regression analyses to determine their prognostic value. We focused on the five most relevant genes (*GOLGA8A*, *KLC3*, *TIGD1*, *NBPF1*, and *SERPINE1*) to construct the prognostic model. Based on the median risk score, we separated the patients into low- and high-risk groups. The patients who died demonstrated greater risk ratings than those who survived, according to the distinct survival stages. Additionally, compared with the low-risk group, the high-risk group demonstrated shorter PFS and OS. Furthermore, we confirmed a good prognostic potential of this gene signature in patients with COAD. The five gene characteristics were the independent predictive models for the patients, according to the univariate and multivariate Cox regression analysis, which included a range of clinically relevant covariates. We used the ROC curve, C-index model, and nomogram to validate the good prognostic value and accuracy of the model.

Based on *GOLGA8A*, *KLC3*, *TIGD1*, *NBPF1*, and *SERPINE1*, the prognostic model was developed. Except for *NBPF1*, which displays low expression in patients with COAD, other proteins were substantially expressed in tumor tissues and associated with a bad prognosis. *TIGD1* is a human-specific gene [45]. Some bioinformatic analyses have associated *TIGD1* with a poor prognosis in patients with CRC; nonetheless, further research is necessary to confirm the underlying mechanism [45,46]. Additionally, an increase in *TIGD1* can lead to CRC proliferation or metastasis *(46,48)*. High *SERPINE1* expression increases CRC migration and invasion and increases the degree of malignancy [47–49]. Its mechanism of action involves facilitating the spread of cancer cells to neighboring healthy tissues, therefore advancing cancer [50]. This phenomenon is a risk factor for people with CRC [49]. Furthermore, it is involved in treating drug-resistant cancers [51,52]. Research has demonstrated that *NBPF1* deficiency causes colorectal cancer and poor survival [53], which appears to corroborate the finding that tumor expression in the findings is lower than in normal tissues.

First, we conducted a mutation correlation analysis on these five gene signatures to investigate their possible biological roles. We observed low mutation frequency, indicating stable gene signatures. Second, we examined the immune function of the model using the "ssGSEA" algorithm. The difference between the high- and low-risk groups was primarily attributed to inflammation-promotion, CCR, APC co-stimulation, check-point, HLA, and parainflammation. The CCR family is a novel target for cancer immunotherapy and immunotherapy [54]. Both cancer cells and stromal cells express homologous receptors for this broad family of cytokines, which have chemotactic action. During the disease, their changed expression in malignant tumors controls angiogenesis, metastasis, leukocyte recruitment, and activation [55,56]. The CCR family can be associated with several signaling pathways, particularly those related to chemotherapeutic resistance and tumor spread [57]. The immunological microenvironment and its associated components are resistant to chemotherapy in tumors [58,59]. Numerous novel therapeutic targets can be used to alleviate tumor immune tolerance because of factors, including the extracellular matrix stress, altered phenotypic and metabolic states of innate immune cells (such as mast cells and neutrophils), and emerging immune tolerance mechanisms mediated by adaptive immune cells in the tumor microenvironment [60]. However, the impact of resistance on the immune microenvironment is unclear. We determined the association between the TIME and 5FRRDEG-based genetic models. The characteristics of immune cell infiltration in patients with COAD were studied using a risk model-based grouping. The low-risk group demonstrated a higher percentage of $CD8^+$ cells, macrophages, and NK cell infiltration. This finding was consistent with the examination of immune-related functions, which suggested a stronger association between inflammatory and parainflammatory functions in the low-risk group.

Our model was correlated with immunological checkpoints; immune escape from tumors was enhanced by its expression, according to an immune-related functional study. Subsequently, we examined the correlations between five genes and the immunological checkpoints *B7H3*, *PDL1*, and *PDL2*. Positive correlations between *KLC3*, *SERPINE1* and *PDL1*, *NBPF1*, *SERPINE1* and *PDL2*, *KLC3*, *SERPINE1* and *B7H3* are discovered. This finding was consistent with higher expression of immunosuppressive genes, which enhance the resistance of tumor cells to host immunosuppression [61,62]. Consequently, the immunological checkpoints were associated with the prognostic model, which may facilitate patient screening, appropriate treatments, and customized care. Furthermore, we assessed the medications frequently prescribed to the patients for targeted therapy and chemotherapy. The low-risk

group was more responsive to the chemo-targeted therapy. In conclusion, this gene model affects the clinical management of patients with COAD.

5. Conclusion

We used a prognostic model based on five 5FRRDEGs to predict the tumor immune state, chemotherapy response, and immunotherapy response in patients with COAD. The model offered a reference value and guided the individualization of therapy in clinical settings. Our findings will offer a direction for future research to examine the mechanism underlying medication resistance in CRC. Furthermore, the signature association with the TIME indicates its use to accurately predict the effectiveness of immunotherapy. However, this study has several limitations. The sample size was insufficient, and the sample type was restricted to patients with COAD. Moreover, we only explored the function from the existing data. Additionally, relevant experiments were absent to confirm the applicable functions.

Data availability statement

The original contributions of the study are contained in the article and Supplementary Material. You can contact the corresponding author with additional queries. Publicly available datasets were analyzed in this study. The data associated with my study has been deposited into a publicly available repository. The data can be found in TCGA (https://portal.gdc.cancer.gov/), the GEO database (https://www.ncbi.nlm.nih.gov/geo/), the HPA (https://www.proteinatlas.org/), the GDSC website (https://www.cancerrxgene.org/), and the TIMER database (http://cistrome.org/TIMER/).

Data associated with my study has been deposited into a publicly available repository.

Funding statement

This work was supported by the Research projects of traditional Chinese medicine of Hunan Province (No. A2023043), Hunan Provincial Clinical Medical Research Center Project (No. 2023SK4048), and Hunan Shennong talent funding project.

CRediT authorship contribution statement

Haixia Yan: Writing – review & editing, Writing – original draft, Data curation, Conceptualization. **Qinling Ou:** Writing – review & editing, Software, Methodology. **Yonglong Chang:** Writing – review & editing, Data curation, Conceptualization. **Jinhui Liu:** Writing – review & editing, Software, Methodology. **Linzi Chen:** Writing – review & editing, Software, Methodology. **Duanyang Guo:** Writing – review & editing, Supervision, Resources. **Sifang Zhang:** Writing – review & editing, Writing – original draft, Data curation.

Declaration of competing interest

The authors declare no conflict of interest.

Acknowledgements

We gratefully acknowledge the Cancer Genome Atlas (TCGA) database, the Gene Expression Omnibus database (GEO), and the Human Protein Atlas (HPA) database, which made the data available, and we would like to express our sincere thanks to all the editors, reviewers, and other staff who participated in reviewing and producing this paper.

Appendix A. Supplementary data

Supplementary data to this article can be found online at https://doi.org/10.1016/j.heliyon.2024.e34535.

References

[1] M. Xu, J. Mu, J. Wang, Q. Zhou, J. Wang, Construction and validation of a cuproptosis-related lncRNA signature as a novel and robust prognostic model for colon adenocarcinoma, Front. Oncol. 12 (2022) 961213, https://doi.org/10.3389/fonc.2022.961213.
[2] E. Dekker, P.J. Tanis, J.L.A. Vleugels, P.M. Kasi, M.B. Wallace, Colorectal cancer, Lancet 394 (2019) 1467–1480, https://doi.org/10.1016/S0140-6736(19)32319-0.
[3] S.G. Patel, D.J. Ahnen, Colorectal cancer in the young, Curr. Gastroenterol. Rep. 20 (2018) 15, https://doi.org/10.1007/s11894-018-0618-9.
[4] M. Valdivieso, G.M. Mavligit, Chemotherapy and chemoimmunotherapy of colorectal cancer. Role of the carcinoembryonic antigen, Surg Clin North Am 58 (1978) 619–631, https://doi.org/10.1016/s0039-6109(16)41543-4.
[5] A.B. Benson, A.P. Venook, M.M. Al-Hawary, L. Cederquist, Y.-J. Chen, K.K. Ciombor, S. Cohen, H.S. Cooper, D. Deming, P.F. Engstrom, I. Garrido-Laguna, J. L. Grem, A. Grothey, H.S. Hochster, S. Hoffe, S. Hunt, A. Kamel, N. Kirilcuk, S. Krishnamurthi, W.A. Messersmith, J. Meyerhardt, E.D. Miller, M.F. Mulcahy, J. D. Murphy, S. Nurkin, L. Saltz, S. Sharma, D. Shibata, J.M. Skibber, C.T. Sofocleous, E.M. Stoffel, E. Stotsky-Himelfarb, C.G. Willett, E. Wuthrick, K.M. Gregory,

D.A. Freedman-Cass, NCCN Guidelines insights: colon cancer, version 2.2018, J. Natl. Compr. Cancer Netw. 16 (2018) 359–369, https://doi.org/10.6004/jnccn.2018.0021.
[6] F.A. Haggar, R.P. Boushey, Colorectal cancer epidemiology: incidence, mortality, survival, and risk factors, Clin. Colon Rectal Surg. 22 (2009) 191–197, https://doi.org/10.1055/s-0029-1242458.
[7] K.D. Miller, L. Nogueira, T. Devasia, A.B. Mariotto, K.R. Yabroff, A. Jemal, J. Kramer, R.L. Siegel, Cancer treatment and survivorship statistics, 2022, CA Cancer J Clin 72 (2022) 409–436, https://doi.org/10.3322/caac.21731.
[8] K. Van der Jeught, H.-C. Xu, Y.-J. Li, X.-B. Lu, G. Ji, Drug resistance and new therapies in colorectal cancer, World J. Gastroenterol. 24 (2018) 3834–3848, https://doi.org/10.3748/wjg.v24.i34.3834.
[9] S. Vodenkova, T. Buchler, K. Cervena, V. Veskrnova, P. Vodicka, V. Vymetalkova, 5-fluorouracil and other fluoropyrimidines in colorectal cancer: past, present and future, Pharmacol. Ther. 206 (2020) 107447, https://doi.org/10.1016/j.pharmthera.2019.107447.
[10] X. Huang, K. Ke, W. Jin, Q. Zhu, Q. Zhu, R. Mei, R. Zhang, S. Yu, L. Shou, X. Sun, J. Feng, T. Duan, Y. Mou, T. Xie, Q. Wu, X. Sui, Identification of genes related to 5-fluorouracil based chemotherapy for colorectal cancer, Front. Immunol. 13 (2022) 887048, https://doi.org/10.3389/fimmu.2022.887048.
[11] S. Blondy, V. David, M. Verdier, M. Mathonnet, A. Perraud, N. Christou, 5-Fluorouracil resistance mechanisms in colorectal cancer: from classical pathways to promising processes, Cancer Sci. 111 (2020) 3142–3154, https://doi.org/10.1111/cas.14532.
[12] X. Wang, G. Jiang, W. Ren, B. Wang, C. Yang, M. Li, LncRNA NEAT1 regulates 5-fu sensitivity, apoptosis and invasion in colorectal cancer through the MiR-150-5p/CPSF4 Axis, OncoTargets Ther. 13 (2020) 6373–6383, https://doi.org/10.2147/OTT.S239432.
[13] Y. Shi, J. Adu-Amankwaah, Q. Zhao, X. Li, Q. Yu, A. Bushi, J. Yuan, R. Tan, Long non-coding RNAs in drug resistance across the top five cancers: update on their roles and mechanisms, Heliyon 10 (2024) e27207, https://doi.org/10.1016/j.heliyon.2024.e27207.
[14] D.C. Hinshaw, L.A. Shevde, The tumor microenvironment innately modulates cancer progression, Cancer Res. 79 (2019) 4557–4566, https://doi.org/10.1158/0008-5472.CAN-18-3962.
[15] M. Binnewies, E.W. Roberts, K. Kersten, V. Chan, D.F. Fearon, M. Merad, L.M. Coussens, D.I. Gabrilovich, S. Ostrand-Rosenberg, C.C. Hedrick, R.H. Vonderheide, M.J. Pittet, R.K. Jain, W. Zou, T.K. Howcroft, E.C. Woodhouse, R.A. Weinberg, M.F. Krummel, Understanding the tumor immune microenvironment (TIME) for effective therapy, Nat Med 24 (2018) 541–550, https://doi.org/10.1038/s41591-018-0014-x.
[16] D.F. Quail, J.A. Joyce, Microenvironmental regulation of tumor progression and metastasis, Nat Med 19 (2013) 1423–1437, https://doi.org/10.1038/nm.3394.
[17] Y. Xiao, D. Yu, Tumor microenvironment as a therapeutic target in cancer, Pharmacol. Ther. 221 (2021) 107753, https://doi.org/10.1016/j.pharmthera.2020.107753.
[18] J.M. Pitt, A. Marabelle, A. Eggermont, J.-C. Soria, G. Kroemer, L. Zitvogel, Targeting the tumor microenvironment: removing obstruction to anticancer immune responses and immunotherapy, Ann. Oncol. 27 (2016) 1482–1492, https://doi.org/10.1093/annonc/mdw168.
[19] L. Del Giacco, C. Cattaneo, Introduction to genomics, Methods Mol. Biol. 823 (2012) 79–88, https://doi.org/10.1007/978-1-60327-216-2_6.
[20] R.M. Sherman, S.L. Salzberg, Pan-genomics in the human genome era, Nat. Rev. Genet. 21 (2020) 243–254, https://doi.org/10.1038/s41576-020-0210-7.
[21] T.K. Attwood, C.J. Miller, Progress in bioinformatics and the importance of being earnest, Biotechnol. Annu. Rev. 8 (2002) 1–54, https://doi.org/10.1016/s1387-2656(02)08003-1.
[22] G. Cui, J. Liu, C. Wang, R. Gu, M. Wang, Z. Sun, F. Wei, Comprehensive analysis of the prognostic signature and tumor microenvironment infiltration characteristics of cuproptosis-related lncRNAs for patients with colon adenocarcinoma, Front. Oncol. 12 (2022) 1007918, https://doi.org/10.3389/fonc.2022.1007918.
[23] M. Xu, J. Mu, J. Wang, Q. Zhou, J. Wang, Construction and validation of a cuproptosis-related lncRNA signature as a novel and robust prognostic model for colon adenocarcinoma, Front. Oncol. 12 (2022) 961213, https://doi.org/10.3389/fonc.2022.961213.
[24] L. Zhong, J. Zhu, Q. Shu, G. Xu, C. He, L. Fang, A prognostic cuproptosis-related LncRNA signature for colon adenocarcinoma, J Oncol 2023 (2023) 5925935, https://doi.org/10.1155/2023/5925935.
[25] J. Ranstam, J.A. Cook, Kaplan-Meier curve, Br. J. Surg. 104 (2017) 442, https://doi.org/10.1002/bjs.10238.
[26] M. Yamauchi, R. Yamaguchi, A. Nakata, T. Kohno, M. Nagasaki, T. Shimamura, S. Imoto, A. Saito, K. Ueno, Y. Hatanaka, R. Yoshida, T. Higuchi, M. Nomura, D. G. Beer, J. Yokota, S. Miyano, N. Gotoh, Epidermal growth factor receptor tyrosine kinase defines critical prognostic genes of stage I lung adenocarcinoma, PLoS One 7 (2012) e43923, https://doi.org/10.1371/journal.pone.0043923.
[27] Z. Sun, T. Li, C. Xiao, S. Zou, M. Zhang, Q. Zhang, Z. Wang, H. Zhan, H. Wang, Prediction of overall survival based upon a new ferroptosis-related gene signature in patients with clear cell renal cell carcinoma, World J. Surg. Oncol. 20 (2022) 120, https://doi.org/10.1186/s12957-022-02555-9.
[28] J. Xu, K. Guo, X. Sheng, Y. Huang, X. Wang, J. Dong, H. Qin, C. Wang, Correlation analysis of disulfidptosis-related gene signatures with clinical prognosis and immunotherapy response in sarcoma, Sci. Rep. 14 (2024) 7158, https://doi.org/10.1038/s41598-024-57594-x.
[29] J. Wu, H. Zhang, L. Li, M. Hu, L. Chen, B. Xu, Q. Song, A nomogram for predicting overall survival in patients with low-grade endometrial stromal sarcoma: a population-based analysis, Cancer Commun. 40 (2020) 301–312, https://doi.org/10.1002/cac2.12067.
[30] F. Lang, J.A. Cornwell, K. Kaur, O. Elmogazy, W. Zhang, M. Zhang, H. Song, Z. Sun, X. Wu, M.I. Aladjem, M. Aregger, S.D. Cappell, C. Yang, Abrogation of the G2/M checkpoint as a chemo sensitization approach for alkylating agents, Neuro Oncol. (2023), https://doi.org/10.1093/neuonc/noad252 noad252.
[31] M.S. Roberts, J.M. Sahni, M.S. Schrock, K.M. Piemonte, K.L. Weber-Bonk, D.D. Seachrist, S. Avril, L.J. Anstine, S. Singh, S.T. Sizemore, V. Varadan, M. K. Summers, R.A. Keri, LIN9 and NEK2 are core regulators of mitotic fidelity that can Be therapeutically targeted to overcome taxane resistance, Cancer Res. 80 (2020) 1693–1706, https://doi.org/10.1158/0008-5472.CAN-19-3466.
[32] S. Morino, T. Mashima, F. Shirai, S. Nagayama, R. Katayama, H. Seimiya, BET protein-dependent E2F pathway activity confers bell-shaped type resistance to tankyrase inhibitors in APC-mutated colorectal cancer, Cancer Lett. 584 (2024) 216632, https://doi.org/10.1016/j.canlet.2024.216632.
[33] L. Wei, Y. Bai, L. Na, Y. Sun, C. Zhao, W. Wang, E2F3 induces DNA damage repair, stem-like properties and therapy resistance in breast cancer, Biochim. Biophys. Acta, Mol. Basis Dis. 1869 (2023) 166816, https://doi.org/10.1016/j.bbadis.2023.166816.
[34] M.-Z. Cheng, B.-B. Yang, Z.-T. Zhan, S.-M. Lin, Z.-P. Fang, Y. Gao, W.-J. Zhou, MACC1 and Gasdermin-E (GSDME) regulate the resistance of colorectal cancer cells to irinotecan, Biochem. Biophys. Res. Commun. 671 (2023) 236–245, https://doi.org/10.1016/j.bbrc.2023.06.002.
[35] T. Y, Z. H, W. Q, F. S, AXL in cancer: a modulator of drug resistance and therapeutic target, J. Exp. Clin. Cancer Res. : CR 42 (2023), https://doi.org/10.1186/s13046-023-02726-w.
[36] Y. Kuang, K. Yang, L. Meng, Y. Mao, F. Xu, H. Liu, Identification and validation of ferroptosis-related biomarkers and the related pathogenesis in precancerous lesions of gastric cancer, Sci. Rep. 13 (2023) 16074, https://doi.org/10.1038/s41598-023-43198-4.
[37] Q. Nie, H. Cao, J. Yang, T. Liu, B. Wang, PI3K/Akt signalling pathway-associated long noncoding RNA signature predicts the prognosis of laryngeal cancer patients, Sci. Rep. 13 (2023) 14764, https://doi.org/10.1038/s41598-023-41927-3.
[38] X. Wang, R.B. Undi, N. Ali, M.M. Huycke, It takes a village: microbiota, parainflammation, paligenosis and bystander effects in colorectal cancer initiation, Dis Model Mech 14 (2021), https://doi.org/10.1242/dmm.048793 dmm048793.
[39] E. Entezar-Almahdi, S. Mohammadi-Samani, L. Tayebi, F. Farjadian, Recent advances in designing 5-fluorouracil delivery systems: a stepping stone in the safe treatment of colorectal cancer, Int J Nanomedicine 15 (2020) 5445–5458, https://doi.org/10.2147/IJN.S257700.
[40] F. Danesh Pouya, Y. Rasmi, M. Nemati, Signaling pathways involved in 5-FU drug resistance in cancer, Cancer Invest. 40 (2022) 516–543, https://doi.org/10.1080/07357907.2022.2055050.
[41] J. Deng, Y. Wang, J. Lei, W. Lei, J.P. Xiong, Insights into the involvement of noncoding RNAs in 5-fluorouracil drug resistance, Tumour Biol 39 (2017) 1010428317697553, https://doi.org/10.1177/1010428317697553.
[42] C. Sethy, C.N. Kundu, 5-Fluorouracil (5-FU) resistance and the new strategy to enhance the sensitivity against cancer: implication of DNA repair inhibition, Biomed. Pharmacother. 137 (2021) 111285, https://doi.org/10.1016/j.biopha.2021.111285.
[43] J.T. Fekete, B. Győrffy, New transcriptomic biomarkers of 5-fluorouracil resistance, Int. J. Mol. Sci. 24 (2023) 1508, https://doi.org/10.3390/ijms24021508.
[44] Y. Garcia-Mayea, C. Mir, F. Masson, R. Paciucci, M.E. Lleonart, Insights into new mechanisms and models of cancer stem cell multidrug resistance, Semin. Cancer Biol. 60 (2020) 166–180, https://doi.org/10.1016/j.semcancer.2019.07.022.

[45] J. Zou, H. Zhang, Z. Wu, W. Hu, T. Zhang, H. Xie, Y. Huang, H. Zhou, TIGD1 is an independent prognostic factor that promotes the progression of colon cancer, Cancer Biother. Radiopharm. (2022), https://doi.org/10.1089/cbr.2022.0052.
[46] G. Zhang, Z. Feng, Q. Zeng, P. Huang, Exploring Cancer Dependency Map genes and immune subtypes in colon cancer, in which TIGD1 contributes to colon cancer progression, Aging (Albany NY) 15 (2023) 6400–6428, https://doi.org/10.18632/aging.204859.
[47] W.-T. Kim, J.-Y. Mun, S.-W. Baek, M.-H. Kim, G.-E. Yang, M.-S. Jeong, S.Y. Choi, J.-Y. Han, M.H. Kim, S.-H. Leem, Secretory SERPINE1 expression is increased by antiplatelet therapy, inducing MMP1 expression and increasing colon cancer metastasis, Int. J. Mol. Sci. 23 (2022) 9596, https://doi.org/10.3390/ijms23179596.
[48] R. Hughes, J. Parry, J. Beynon, G. Jenkins, Molecular changes consistent with increased proliferation and invasion are common in rectal cancer, Clin. Transl. Oncol. 13 (2011) 753–759, https://doi.org/10.1007/s12094-011-0728-4.
[49] G. Mazzoccoli, V. Pazienza, A. Panza, M.R. Valvano, G. Benegiamo, M. Vinciguerra, A. Andriulli, A. Piepoli, ARNTL2 and SERPINE1: potential biomarkers for tumor aggressiveness in colorectal cancer, J. Cancer Res. Clin. Oncol. 138 (2012) 501–511, https://doi.org/10.1007/s00432-011-1126-6.
[50] Y. Wang, J. Wang, J. Gao, M. Ding, H. Li, The expression of SERPINE1 in colon cancer and its regulatory network and prognostic value, BMC Gastroenterol. 23 (2023) 33, https://doi.org/10.1186/s12876-022-02625-y.
[51] M.A. Pavón, I. Arroyo-Solera, M.V. Céspedes, I. Casanova, X. León, R. Mangues, uPA/uPAR and SERPINE1 in head and neck cancer: role in tumor resistance, metastasis, prognosis and therapy, Oncotarget 7 (2016) 57351–57366, https://doi.org/10.18632/oncotarget.10344.
[52] Q. Zhang, L. Lei, D. Jing, Knockdown of SERPINE1 reverses resistance of triple-negative breast cancer to paclitaxel via suppression of VEGFA, Oncol. Rep. 44 (2020) 1875–1884, https://doi.org/10.3892/or.2020.7770.
[53] R. Ma, C. Jing, Y. Zhang, H. Cao, S. Liu, Z. Wang, D. Chen, J. Zhang, Y. Wu, J. Wu, J. Feng, The somatic mutation landscape of Chinese Colorectal Cancer, J. Cancer 11 (2020) 1038–1046, https://doi.org/10.7150/jca.37017.
[54] S. Raza, S. Rajak, A. Tewari, P. Gupta, N. Chattopadhyay, R.A. Sinha, B. Chakravarti, Multifaceted role of chemokines in solid tumors: from biology to therapy, Semin. Cancer Biol. 86 (2022) 1105–1121, https://doi.org/10.1016/j.semcancer.2021.12.011.
[55] J. Korbecki, S. Grochans, I. Gutowska, K. Barczak, I. Baranowska-Bosiacka, CC chemokines in a tumor: a review of pro-cancer and anti-cancer properties of receptors CCR5, CCR6, CCR7, CCR8, CCR9, and CCR10 ligands, Int. J. Mol. Sci. 21 (2020) 7619, https://doi.org/10.3390/ijms21207619.
[56] V. Mollica Poeta, M. Massara, A. Capucetti, R. Bonecchi, Chemokines and chemokine receptors: new targets for cancer immunotherapy, Front. Immunol. 10 (2019) 379, https://doi.org/10.3389/fimmu.2019.00379.
[57] Z. Tu, R. Xiao, J. Xiong, K.M. Tembo, X. Deng, M. Xiong, P. Liu, M. Wang, Q. Zhang, CCR9 in cancer: oncogenic role and therapeutic targeting, J. Hematol. Oncol. 9 (2016) 10, https://doi.org/10.1186/s13045-016-0236-7.
[58] F. Exposito, M. Redrado, M. Houry, K. Hastings, M. Molero-Abraham, T. Lozano, J.L. Solorzano, J. Sanz-Ortega, V. Adradas, R. Amat, E. Redin, S. Leon, N. Legarra, J. Garcia, D. Serrano, K. Valencia, C. Robles-Oteiza, G. Foggetti, N. Otegui, E. Felip, J.J. Lasarte, L. Paz-Ares, J. Zugazagoitia, K. Politi, L. Montuenga, A. Calvo, PTEN loss confers resistance to anti-PD-1 therapy in non-small cell lung cancer by increasing tumor infiltration of regulatory T cells, Cancer Res. 83 (2023) 2513–2526, https://doi.org/10.1158/0008-5472.CAN-22-3023.
[59] N. Han, H. Wada, T. Kobayashi, R. Otsuka, K.-I. Seino, A mechanism of IL-34-induced resistance against cytotoxic anti-cancer therapies such as radiation by X-ray and chemotherapy by Oxaliplatin, OncoImmunology 12 (2023) 2238499, https://doi.org/10.1080/2162402X.2023.2238499.
[60] Y. Liu, C. Li, Y. Lu, C. Liu, W. Yang, Tumor microenvironment-mediated immune tolerance in development and treatment of gastric cancer, Front. Immunol. 13 (2022) 1016817, https://doi.org/10.3389/fimmu.2022.1016817.
[61] H.O. Alsaab, S. Sau, R. Alzhrani, K. Tatiparti, K. Bhise, S.K. Kashaw, A.K. Iyer, PD-1 and PD-L1 checkpoint signaling inhibition for cancer immunotherapy: mechanism, combinations, and clinical outcome, Front. Pharmacol. 8 (2017) 561, https://doi.org/10.3389/fphar.2017.00561.
[62] Y. Diesendruck, I. Benhar, Novel immune check point inhibiting antibodies in cancer therapy-Opportunities and challenges, Drug Resist Updat 30 (2017) 39–47, https://doi.org/10.1016/j.drup.2017.02.001.